Available online at www.sciencedirect.com

ScienceDirect

Advances in Space Research 38 (2006) 456–460

ADVANCES IN SPACE RESEARCH
(a COSPAR publication)

www.elsevier.com/locate/asr

Why are there stationary EIT wave fronts

P.F. Chen [a,*], C. Fang [a], K. Shibata [b]

[a] *Department of Astronomy, Nanjing University, No. 22 Hankou Road, Nanjing, Jiangsu 210093, China*
[b] *Kwasan Observatory, Kyoto University, Kyoto 607-8471, Japan*

Received 30 October 2004; received in revised form 20 January 2005; accepted 21 January 2005

Abstract

EIT waves are often observed to be propagating EUV enhancements followed by an expanding dimming region after the launch of CMEs. It was widely assumed that they are the coronal counterparts of the chromospheric Moreton waves, though the former are three or more times slower. The existence of a stationary "EIT wave" front in some events, however, posed a big challenge to the wave explanation. Simulations are performed to reproduce the stationary "EIT wave" front, which is exactly located near the footpoint of the magnetic separatrix, consistent with observations. The formation of the stationary front is explained in the framework of our model where "EIT waves" are supposed to be generated by successive opening of the field lines covering the erupting flux rope in CMEs.

Keywords: Coronal mass ejections; Waves; Numerical simulations

1. Introduction

"EIT waves" are usually observed by EUV Imaging Telescope (EIT) on SOHO spacecraft, typically in the running difference images of Fe XII 195 Å, as emission-enhanced arcs propagating from the eruption sites to a large distance in the quiet region after the launch of a CME (Thompson et al., 1998). When the global magnetic structure is simple, they appear as almost circular fronts propagating until the boundary of coronal holes. Otherwise, they generally propagate in the regions that are devoid of magnetic neutral lines and strong magnetic fields (Thompson et al., 1999). The propagation velocities of "EIT waves" range from 170 to 350 km s^{-1}, with a mean velocity of 271 km s^{-1}, which is significantly larger than the sound speed of the plasma emitting the Fe XII 195 Å line (Klassen et al., 2000). Moreover, "EIT waves" are seen to propagate across the solar disk, hence, more or less perpendicular to the magnetic field lines. Therefore, it was widely believed that they are fast-mode magnetoacoustic waves. The hypothesis was backed by the model simulation of Wang (2000) and numerical simulations of Wu et al. (2001) and Li et al. (2002). Since Moreton waves, discovered in Hα more than 40 years ago (Moreton and Ramsey, 1960), were successfully explained by the coronal fast-mode wave (or shock wave) model by Uchida (1968), it was then believed that the observed "EIT waves" are just the coronal counterparts of the chromospheric Moreton waves, which is favored by the occasional cospatiality of a sharp EUV wave front and a Moreton wave front (e.g., Warmuth et al., 2001; Vršnak et al., 2002). However, it is a little difficult for such a wave model of "EIT waves" to explain the velocity discrepancy between Moreton waves and the mostly observed diffuse EIT waves since the former are statistically three or more times faster than the latter. A more serious challenge for the wave model was posed by the discovery of a stationary "EIT wave" front in some events by Delannée and Aulanier (1999)

---

[*] Corresponding author. Tel.: +86 25 83594651; fax: +86 25 83235192.
E-mail address: chenpf@nju.edu.cn (P.F. Chen).
URL: http://astronomy.nju.edu.cn/~chenpf/ (P.F. Chen).

0273-1177/$30 © 2005 COSPAR. Published by Elsevier Ltd. All rights reserved.
doi:10.1016/j.asr.2005.01.049

and Delannée (2000), who showed that some "EIT waves" propagate initially, and then stop to form a stationary front near the place where the magnetic separatrix is rooted. They proposed that the "EIT waves" should not be real waves and could be associated with magnetic rearrangement. By performing numerical simulations of the eruption of a flux rope system with a bipolar magnetic background, Chen et al. (2002) investigated the wave phenomena during CMEs. It was found that the piston-driven shock straddling over the flux rope could correspond to the coronal counterparts of Hα Moreton waves, or the observed sharp EUV wave fronts, whereas another wave-like structure, which propagates behind the coronal Moreton waves with a velocity $\sim$3 times slower, could account for the diffuse "EIT waves". The model was supported by the delicate observations by Harra and Sterling (2003) and Foley et al. (2003).

The interaction between an "EIT wave" and an active region was first simulated by Ofman and Thompson (2002), who assumed the "EIT wave" as a fast magnetoacoustic wave. This paper extends our previous simulations to study the interaction between the "EIT waves" and active regions, with the purpose to demonstrate where and how the stationary wave front can be formed. Note that in this paper the term "EIT wave" is used to mention the diffuse EUV wave fronts, and "coronal Moreton wave" is to the sharp EUV wave fronts.

2. Numerical method

Two-dimensional MHD equations in Cartesian coordinates are numerically solved with a multistep implicit scheme. Independent variables are density (ρ), velocity (v_x, v_y), magnetic flux function (ψ), and temperature (T), note that the magnetic field is related to ψ by $\vec{B} = \vec{\nabla} \times \psi \hat{\mathbf{e}}_z$. The units of all the quantities are the same as in Chen et al. (2002).

The background part of the initial magnetic field used in Chen et al. (2002) is bipolar. To study the interaction between "EIT waves" and active regions, two cases are simulated here, where the active region has a polarity orientation opposite to (case A) and the same as (case B) that of the background field, as shown by Fig. 1. The magnetic component of the active regions reads as follows with ± signs, where '+' is for case A, and '–' for case B:

$$\psi = \pm 0.5 \ln \frac{[(x+4)^2 + (y+0.3)^2][(x+6)^2 + (y+0.3)^2]}{[(x+4.8)^2 + (y+0.3)^2][(x+5.2)^2 + (y+0.3)^2]} \pm 0.5 \ln \frac{[(x-4)^2 + (y+0.3)^2][(x-6)^2 + (y+0.3)^2]}{[(x-4.8)^2 + (y+0.3)^2][(x-5.2)^2 + (y+0.3)^2]}. \tag{1}$$

The inner-most separatrix is just near the boundary of the side active regions in case A, while it is in the midst between the central and the side active regions. A uniform temperature $T = 1$ is assumed. The density is distributed in order that the initial gas pressure can balance the magnetic force within the flux rope when the image current and the background field are absent.

The dimensionless size of the simulation box is $|x| \leqslant 12$ and $0 \leqslant y \leqslant 18$. Owing to symmetry, the simulations are made only in the right half region, which is discretized by 148×541 grid points. To initiate CMEs, shearing motion, converging motion, or flux emergence is appropriate. Here, similar to that in Chen et al. (2002), an upward external force $\vec{F} = [1.3 + 5.7(v_{\rm rope} - v_{\rm c})/v_{\rm rope}]\mathrm{e}^{4(\psi_{\rm c}-\psi)}\vec{\mathrm{e}}_y$ is exerted on the flux rope, i.e., the region with $-1.5 \geqslant \psi \geqslant \psi_{\rm c}$, where $\psi_{\rm c}$ is the value of ψ at the flux rope center, $v_{\rm c}$ is the velocity at the flux rope center, and $v_{\rm rope} = 100$ km s^{-1}.

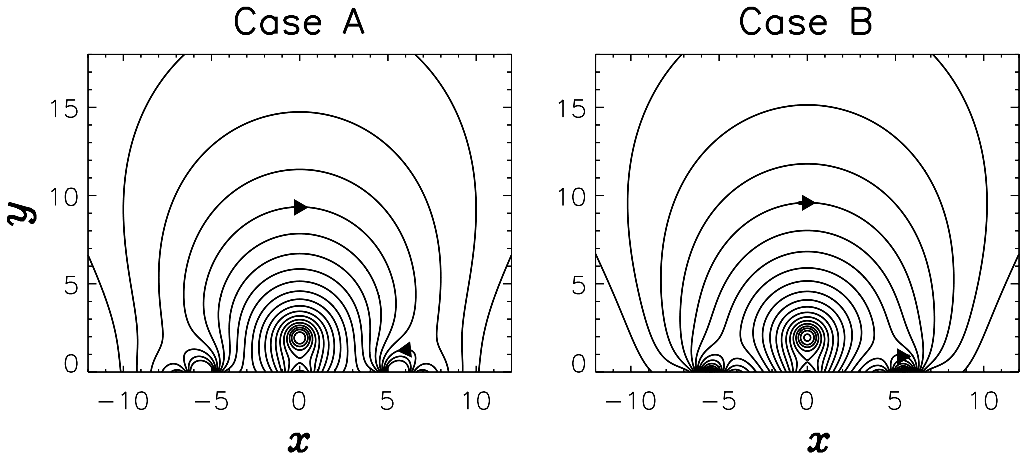

Fig. 1. Initial Magnetic configurations in case A (left panel) and case B (right panel).

3. Numerical results

The early evolution in the two cases is similar to that described in Chen et al. (2002), i.e., after the introduction of the driving force, the flux rope is ejected to produce a CME. Below the flux rope, the plasma is evacuated so that the lateral plasma with frozen-in field lines is driven inward; at the same time, the antiparallel field lines are stretched. Therefore, the initial magnetic null point evolves into a current sheet, where magnetic reconnection occurs. Below the reconnection X-point, cusp-shaped flare loops are formed. The erupting flux rope also pulls up the closed field lines to expand, by which a piston-driven shock appears straddling over the CME. The shock extends down to the solar surface, though the strength decreases from the top to the low ends. As the piston-driven shock propagates outward, its legs sweep the solar surface with a super-Alfvén velocity, which were explained as the coronal counterparts of chromospheric Moreton waves, and may be called coronal Moreton waves. Simultaneously, another wave-like structure bordering an expanding plasma-depleted region propagates behind the coronal Moreton wave with a propagation velocity three times smaller, which was explained to correspond to the observed "EIT wave" by Chen et al. (2002).

When the coronal Moreton wave approaches the active region, which is embedded in an otherwise bipolar background field, it is deflected upward by the strong magnetic field to stride it rapidly in both cases. In contrast, when the "EIT wave" gets closer to the boundary of the active region, its propagation speed decreases rapidly in case A and weakly in case B. However, in both cases, a stationary "EIT wave" front is formed near the footpoint of the magnetic separatrix, which is near $x = 4.8$ in case A and $x = 3$ in case B, as indicated in Fig. 2.

4. Discussions

Recent observations show more and more evidence indicative of the non-wave nature of the diffuse "EIT waves" (see Chen et al., 2005, and references therein). Among them, the discovery of a stationary "EIT wave" front in some events posed a big challenge to the fast-mode wave explanation for the phenomenon (Delannée and Aulanier, 1999; Delannée, 2000). The research by Chen et al. (2002) revealed that two wave-like phenomena are associated with CMEs, i.e., the sharp coronal Moreton waves and the diffuse "EIT waves". In this paper, we extend the previous modeling to study the interaction between these waves and active regions. Two cases are simulated, where the polarity orientation of the active region is opposite to that of the background field in case A, and the same in case B. The numerical results show quite similar evolutions in the two cases. When the Moreton wave approaches the active region with a super-Alfvén speed, it is deflected upward to stride the strong magnetic structure in both cases. However, when the "EIT wave" approaches the active region with a slower speed, it is decelerated rapidly in case A, and eventually stop to form a stationary front near the footpoint of the separatrix at $x = 4.8$. In case B, the "EIT wave" shows weak deceleration, and then stop suddenly to form a stationary front near the footpoint of the separatrix at $x = 3$. The above evolution in the two cases and in particular their difference can be understood as follows. According to the "EIT wave" model of Chen et al. (2002), coronal Moreton waves correspond to the piston-driven shock straddling over the erupting flux rope. As the common nature of waves, they would be deflected by strong magnetic structures, and be seen to circumvent or stride the structures with significantly weakened amplitude. This is why Moreton waves are observable only in the regions with weak magnetic field. On the

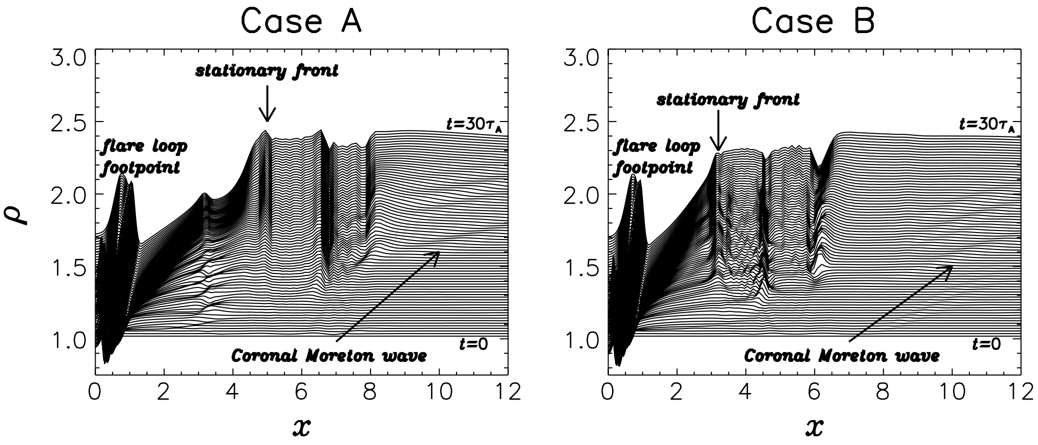

Fig. 2. Evolution of the density (ρ) distribution along the line $y = 0.5$ in case A (left panel) and case B (right panel). Note that the ρ distribution at each time is stacked on the previous one with an increment of 0.018 for every $0.4\tau_A$.

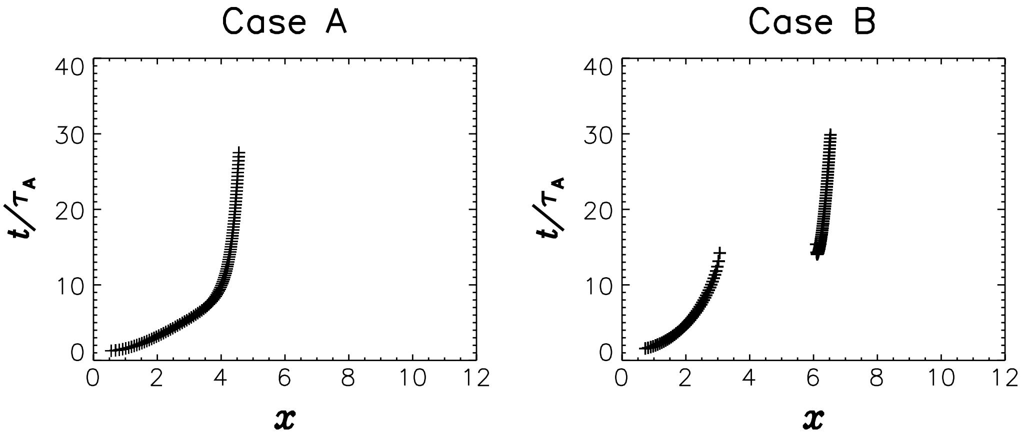

Fig. 3. Theoretical estimate of the "EIT wave" progression in case A (left panel) and case B (right panel) based on the model of Chen et al. (2002).

other hand, "EIT waves" are generated by successive opening of closed field lines covering the erupting flux rope, where the perturbations with large-amplitude originating from the erupting flux rope propagate upward to the top of each field line, and then downward along the field line to the footpoint. If the field lines are approximately semicircle-shaped, it is found that the "EIT wave" speed is about one-third of the in situ fast-mode wave speed (Chen et al., 2002). However, the field lines in case A are strongly convergent toward the footpoint of the separatrix at $x = 4.8$ near the boundary of the active region, which has a polarity orientation opposite to that of the background field. Therefore, when the "EIT wave" approaches the footpoint of the separatrix, the progression of the "EIT wave" gets smaller and smaller for the same time interval, i.e., the apparent velocity of the "EIT wave" becomes smaller and smaller. This is consistent with the analytic solution of the "EIT wave" progression for the initial magnetic configuration in case A, as shown by the left panel of Fig. 3, which is calculated based on the "EIT wave" model of Chen et al. (2002). Eventually, when the field line just close to the separatrix is stretched, it keeps pressing the active region to form a stationary front with enhanced density. In case B, the field lines are much less convergent toward the footpoint of the separatrix at $x = 3$ in front of the active region, which has the same polarity orientation as that of the background field. Correspondingly, the "EIT wave" velocity keeps large with weak deceleration until the wave front approaches the separatrix as shown by the right panel of Fig. 3. However, similarly to in case A, when the field line just close to the separatrix is stretched, it also keeps pressing the active region so that a stationary front would be formed. It is also seen from Fig. 2 that stationary fronts exist at other feet of the separatrices as well, which have not been observed, possibly owing to their fainter emission. Note that "EIT wave" front may reappear on the outer edge of the active region (near $x = 6$) as shown by both the numerical results and the analytic solution in case B. In case A, this happens much later, and is not shown in Fig. 3.

To summarize, the existence of a stationary "EIT wave" front, which is near the footpoint of the magnetic separatrix, is strongly indicative of the non-wave nature of the diffuse "EIT wave" phenomenon. It can be explained by the "EIT wave" model of Chen et al. (2002), and is reproduced by the numerical simulations in this paper. Since the boundary of coronal holes is also a separatrix, it is not surprising that "EIT waves" generally stop near the boundary of coronal holes, as revealed by observations (Thompson et al., 1999). Part of our numerical results, i.e., the interaction between the Moreton wave and an active region, is quite similar to that in Ofman and Thompson (2002), who simulated the interaction between a fast magnetoacoustic wave and an active region.

Acknowledgments

The authors thank two referees for their helpful suggestions. The research is supported by FANEDD (200226), NSFC (10221001, 10333040 and 10403003) and NKBRSF (G20000784).

References

Chen, P.F., Fang, C., Shibata, K. A full view of EIT wave, ApJ, 2005 (in press).

Chen, P.F., Wu, S.T., Shibata, K., Fang, C. Evidence of EIT and Moreton waves in numerical simulations. ApJ 572, L99–L102, 2002.

Delannée, C. Another view of the EIT wave phenomenon. ApJ 545, 512–523, 2000.

Delannée, C., Aulanier, G. CME associated with transequatorial loops and a bald patch flare. Solar Phys. 190, 107–129, 1999.

Foley, C.R., Harra, L.K., Matthews, S.A., Culhane, J.L., Kitai, R. Evidence for a flux rope driven EUV wave and CME: comparison with the piston shock model. A&A 399, 749–754, 2003.

Harra, L.K., Sterling, A.C. Imaging and spectroscopic investigations of a solar coronal wave. ApJ 587, 429–438, 2003.

Klassen, A., Aurass, H., Mann, G., Thompson, B.J. Catalogue of the 1997 SOHO-EIT coronal transient waves and associated type II radio burst spectra. A&A Suppl. 141, 357–369, 2000.

Li, B., Zheng, H.N., Wang, S. Propagation of disturbances in the solar chromosphere and corona. Chinese Astron. Astrophys. 26, 458–468, 2002.

Moreton, G.E., Ramsey, H.E. Recent observations of dynamical phenomena associated with solar flares. PASP 72, 357, 1960.

Ofman, L., Thompson, B.J. Interaction of EIT waves with coronal active regions. ApJ 574, 440–452, 2002.

Thompson, B.J., Gurman, J.B., Neupert, W.M., et al. SOHO/EIT observations of the 1997 April 7 coronal transient: possible evidence of coronalMoreton waves. ApJ 517, L151–L154, 1999.

Thompson, B.J., Plunkett, S.P., Gurman, J.B., et al. SOHO/EIT observations of an Earth-directed CME on May 12,1997, 1998. Geophys. Res. Lett. 25, 2465–2468, 1998.

Uchida, Y. Propagation of hydromagnetic disturbances in the solar corona and Moreton's wave phenomenon. Solar Phys. 4, 30–44, 1968.

Vršnak, B., Warmuth, A., Brajša, R., Hanslmeier, A. Flare waves observed in Helium I 10830 Å. A&A 394, 299–310, 2002.

Wang, Y.-M. EIT waves and fast-mode propagation in the solar corona. ApJ 543, L89–L93, 2000.

Warmuth, A., Vrsnak, B., Aurass, H., Hanslmeier, A. Evolution of two EIT/H α moreton wave. ApJ 560, L105–L109, 2001.

Wu, S.T., Zheng, H.N., Wang, S., et al. Three-dimensional numerical simulation of MHD waves observed by the EIT. J. Geophys. Res. 106, 25089–25102, 2001.